EUROGRAPHICS 2021 / N. Mitra and I. Viola
(Guest Editors)

Volume 40 (2021), Number 2

Supplemental Material - Honey, I Shrunk the Domain: Frequency-aware Force Field Reduction for Efficient Fluids Optimization

Jingwei Tang[1], Vinicius C. Azevedo[1], Guillaume Cordonnier[1,2] and Barbara Solenthaler[1]

[1]ETH Zürich [2]Inria, Université Côte d'Azur

1. Extended Results

Addtional results of the 2-D test cases are shown in Figures 1, 2, 3, 4, 5, 6, 7, 8, 9. In these figures, we compare the results of ours with the methods of Baseline, Baseline w/ TV, Progressive Upsampling, and Ours w/o Ψ. The experiments are performed on *uniform force*, *S-shaped force* and *multi-vortex force* examples at resolutions 64^2, 128^2 and 256^2. Both *uniform force* and *multi-vortex force* examples are the same examples from the main text. *S-shaped force* example serves as an extra 2-D benchmark test. It is generated by two flat Gaussians ($\sigma x >> \sigma y$) on the upper and lower part of the scene, resulting in roughly three main shearing forces. When Baseline method is applied on the *multi-vortex force* example at resolutions 128^2 and 256^2, it diverges after a few iterations. Therefore, the results are not shown. Additionally, we show the convergence plots of all above optimization schemes under the results of each example.

The method of Baseline has already converged to a bad local minimum at at resolution 64^2 (Figures 1, 4). When TV regularization is used, Baseline w/ TV can converge to a better minima in these lower resolution settings. However, when Baseline w/ TV is applied to higher resolutions 128^2 and 256^2, it still converges badly (Figures 2, 3, 6). Strategies of Progressive Upsampling and Ours w/o Ψ improve upon Baseline w/ TV in higher resolution settings. But they still perform worse than our method (Figures 3, 6, 9). The convergence plot also shows the advantage of our method in convergence speed, especially in *multi-vortex force* example shown in Figures 1, 2, 3.

Different optimization schemes are also evaluated on the 3-D *twist* example in Figure 11. Both methods of Baseline and Baseline w/ TVfail to match the keyframes properly. Progressive Upsampling method improves the keyframe matching, but generates overly-turbulent transition frames. Ours w/o Ψ method generates smoother transitions, but fails to match keyframe 11. Our method can match all the keyframes well and generates smooth transition frames. The convergence plot of the 3-D *twist* example is shown in Figure 10. The method of Baseline, Progressive Upsampling and Ours w/o Ψget stuck in bad local minimum at an early stage while the method of Baseline w/ TV converges very slowly. Although our method converges slightly slower than Baseline, Progressive Upsampling and Ours w/o Ψ, but to a much better minima.

Additionally, extended 3-D results of low frequency previews for *soft punch* and *dragon* examples are shown in Figure 12 and 13 respectively. The corresponding cutoff wavenumber k's are 1, 3, 8, 23, 64 for each row. The runtime for *soft punch* example in Figure 12 are 166, 333, 500, 663 and 824 minutes respectively for each wavenumber. The runtime for *soft punch* example in Figure 13 are 74, 318, 557, 794 and 1028 minutes respectively for each wavenumber.

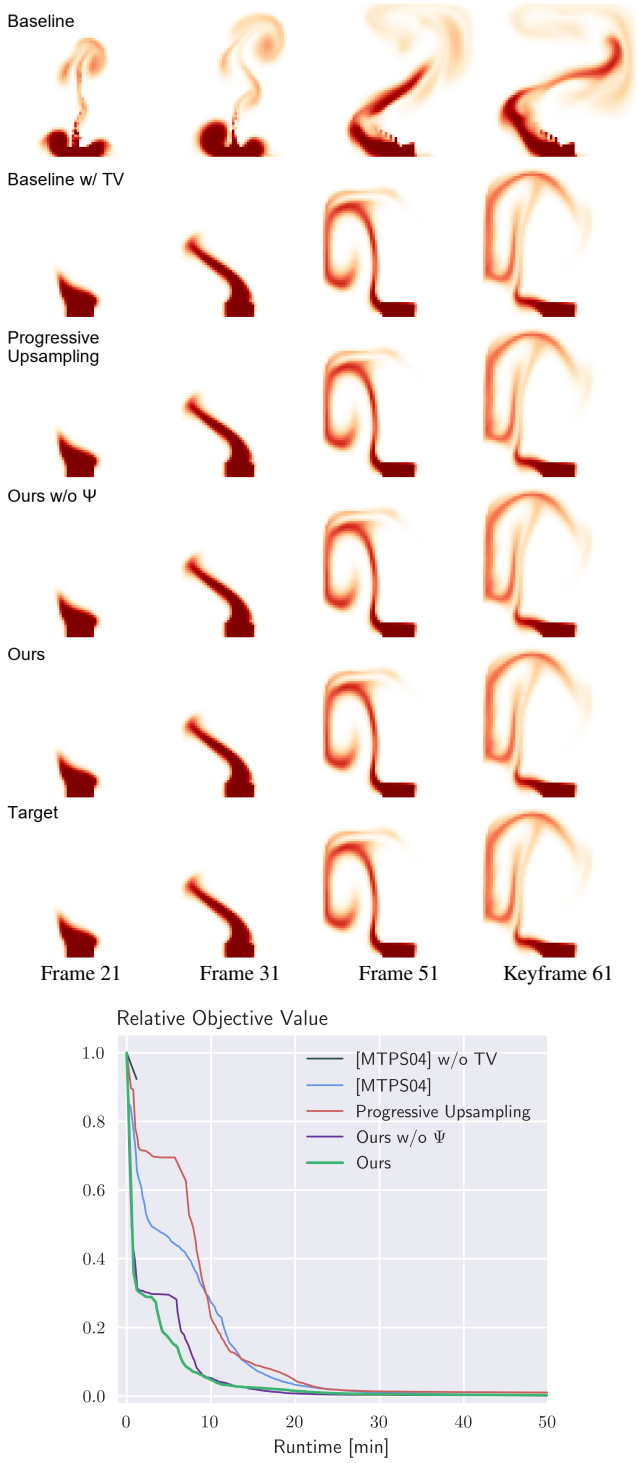

Figure 1: *multi-scale vortex force* example at resolution 64^2 for different optimization schemes. 6 keyframes are used for this example. Only 4 of them are shown.

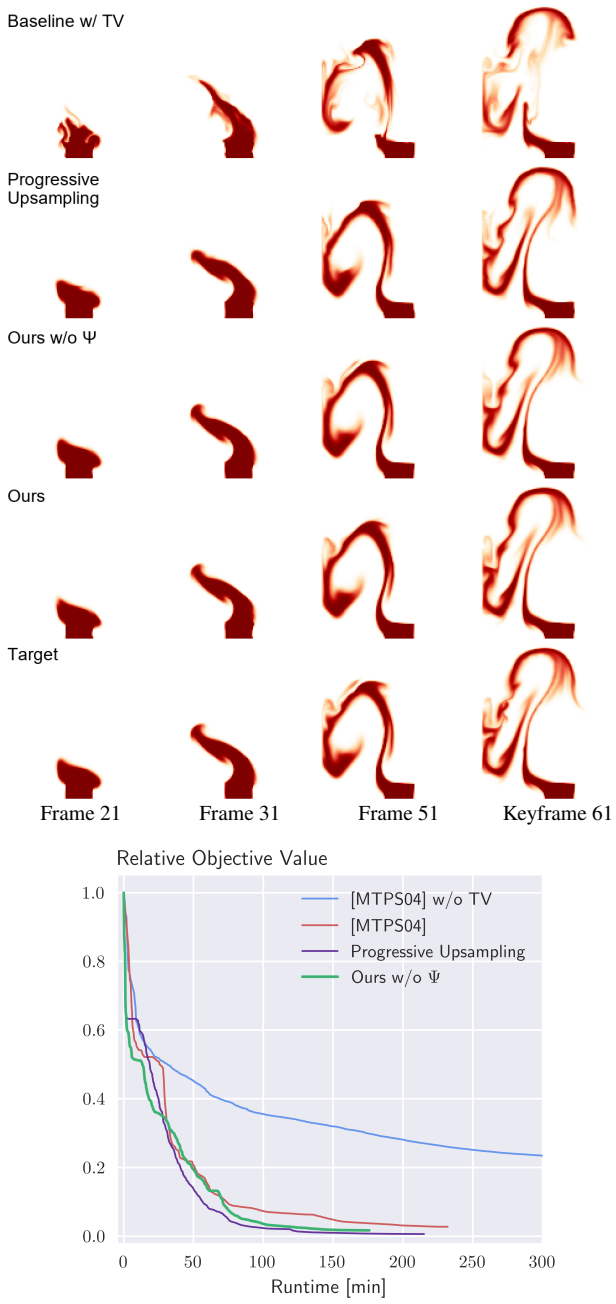

Figure 2: *multi-scale vortex force* example at resolution 128^2 for different optimization schemes. The method of Baseline diverges after a few optimization iterations, thus not shown.

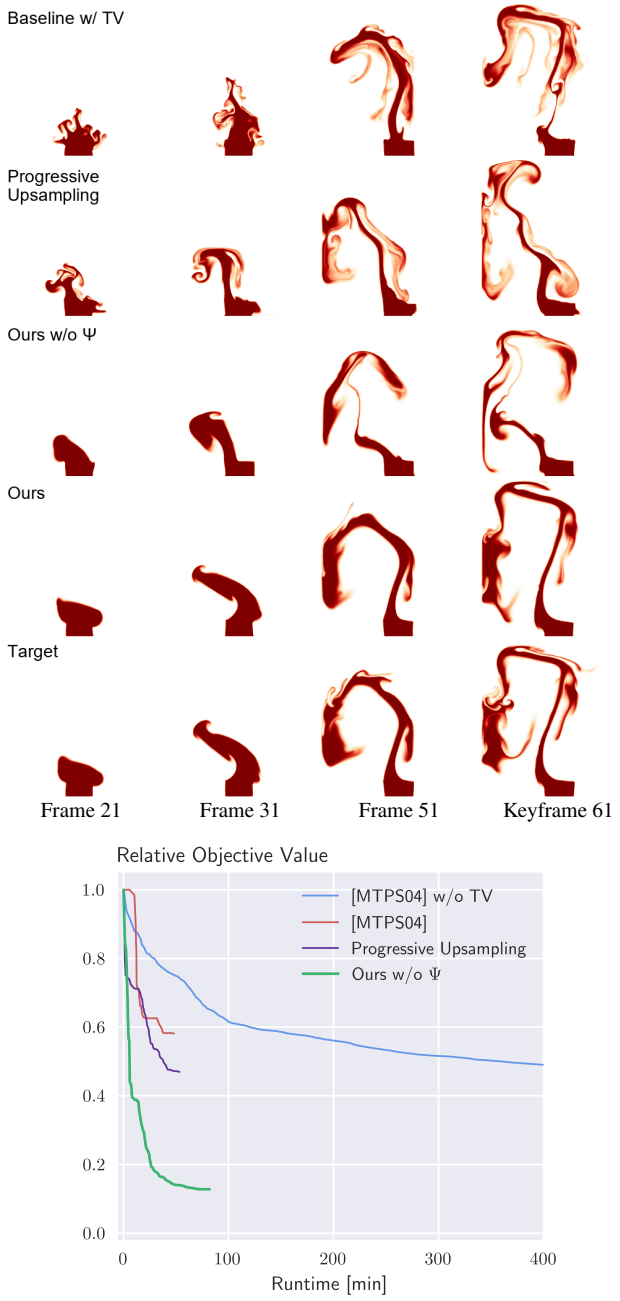

Figure 3: *multi-scale vortex force* example at resolution 256^2 for different optimization schemes. The method of Baseline diverges after a few optimization iterations, thus not shown.

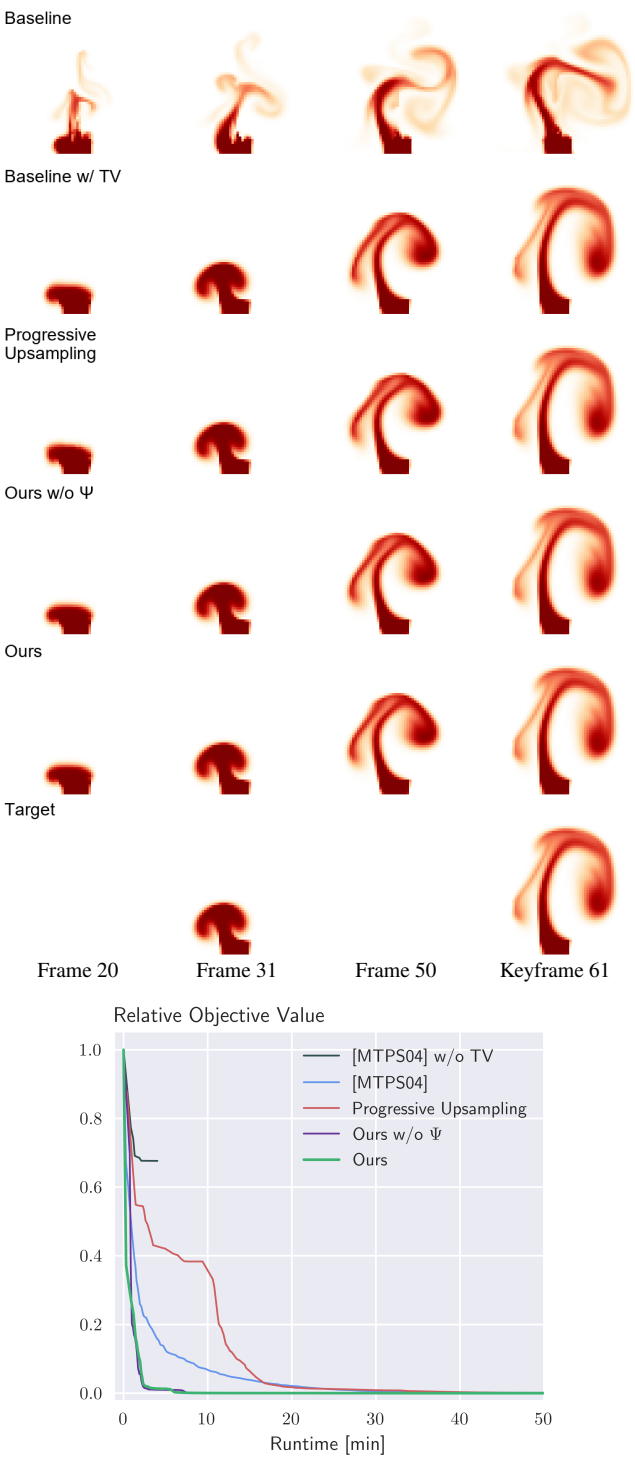

Figure 4: *S-shaped force* example at resolution 64^2 for different optimization schemes.

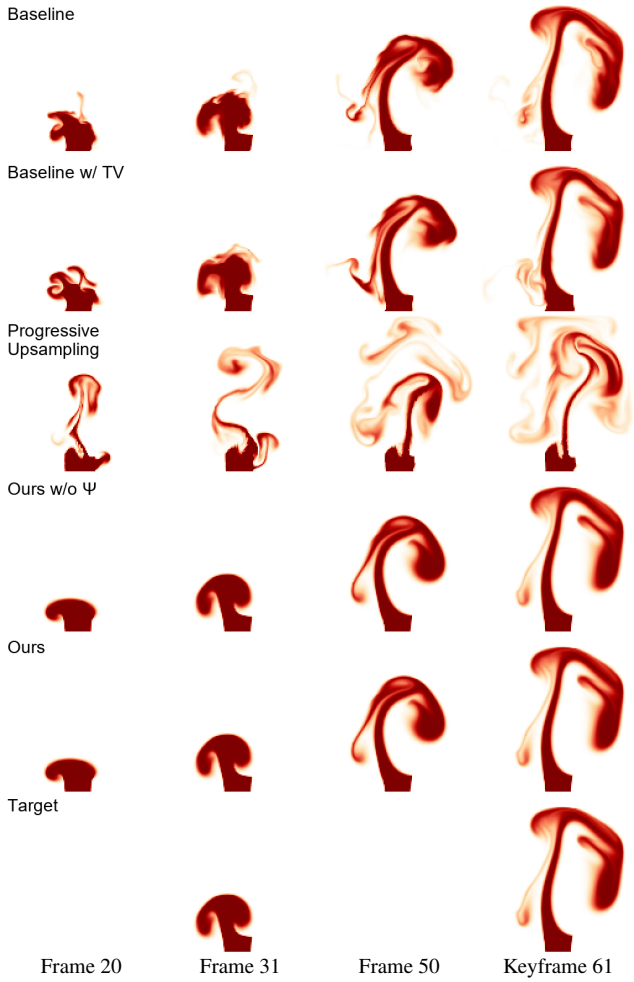

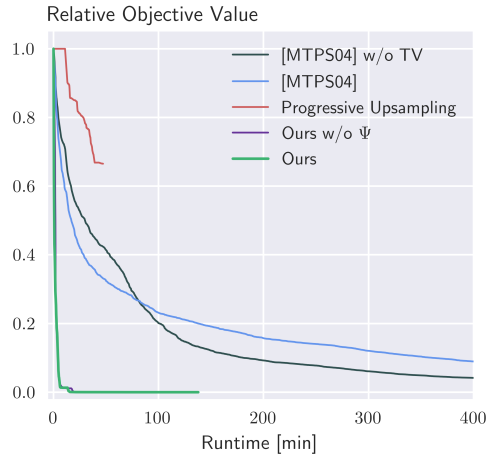

Figure 5: *S-shaped force* example at resolution 128^2 for different optimization schemes.

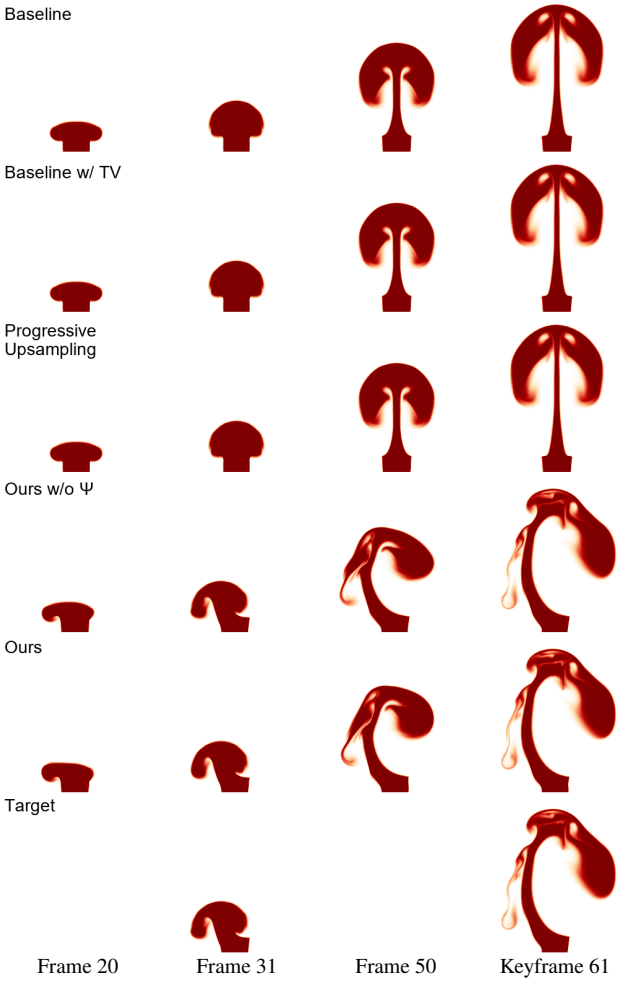

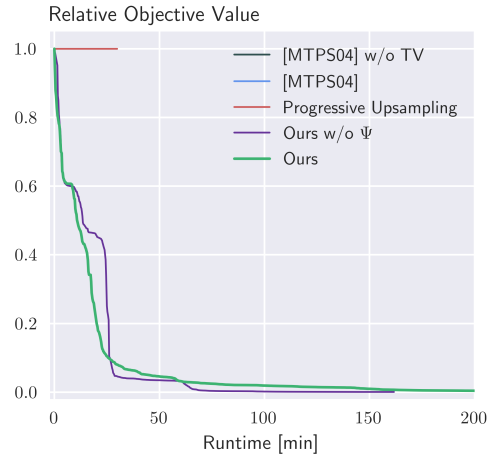

Figure 6: *S-shaped force* example at resolution 256^2 for different optimization schemes.

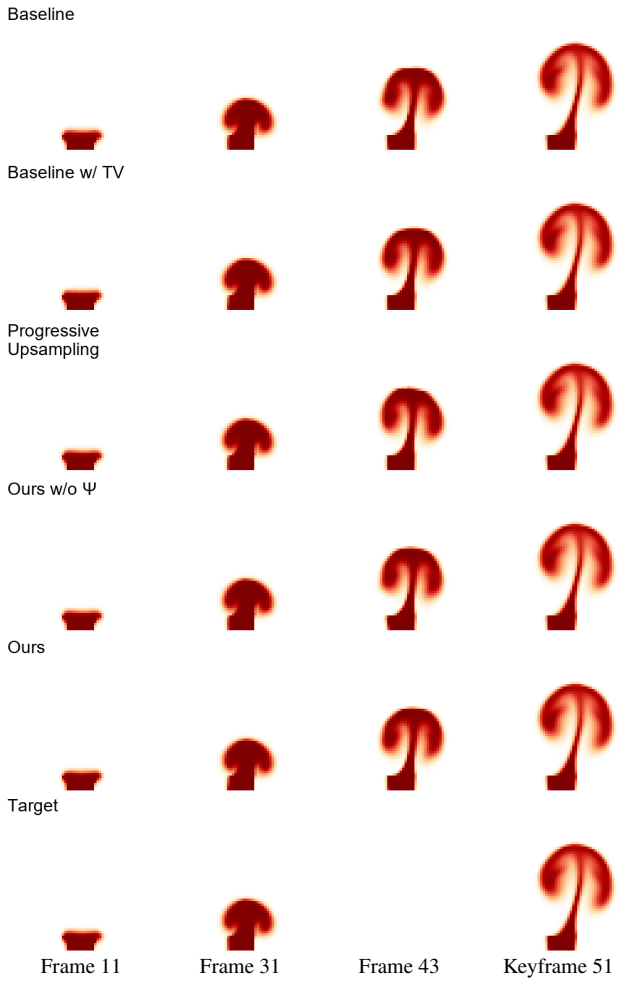

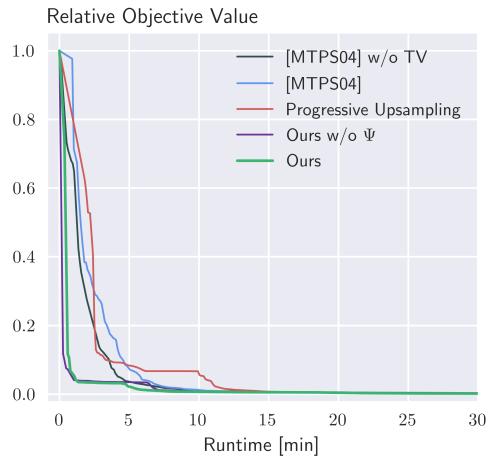

Figure 7: *uniform force* example at resolution 64^2 for different optimization schemes.

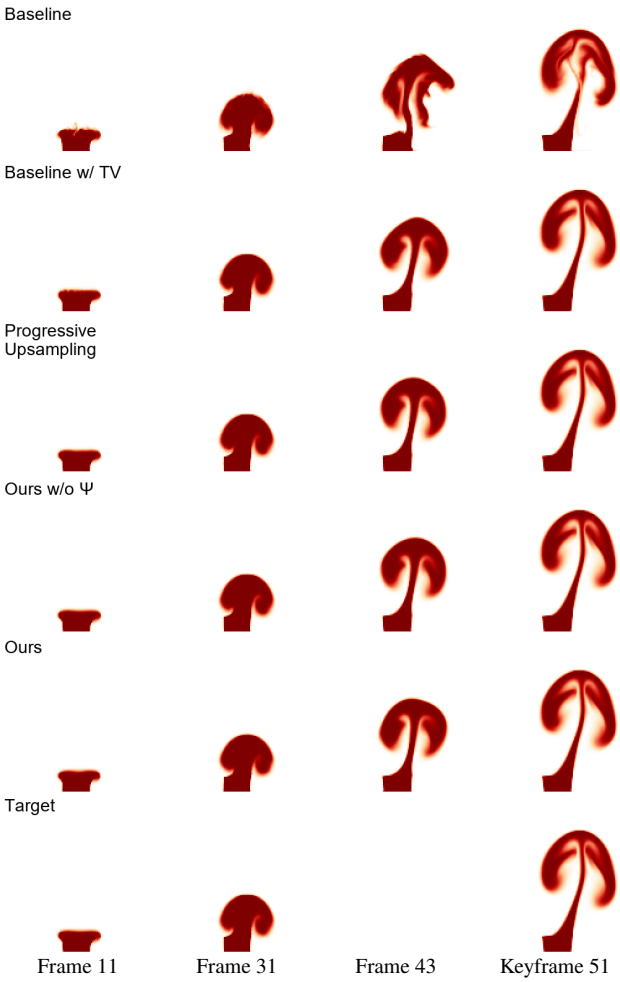

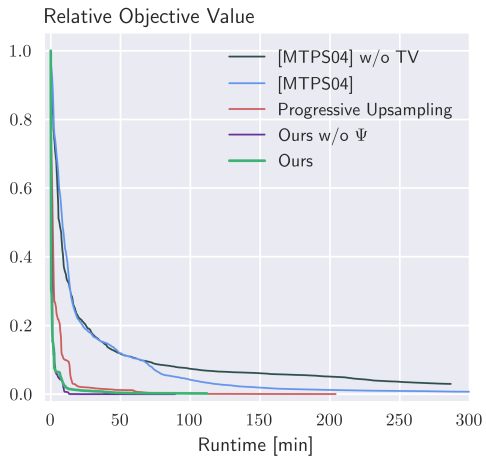

Figure 8: *uniform force* example at resolution 128^2 for different optimization schemes.

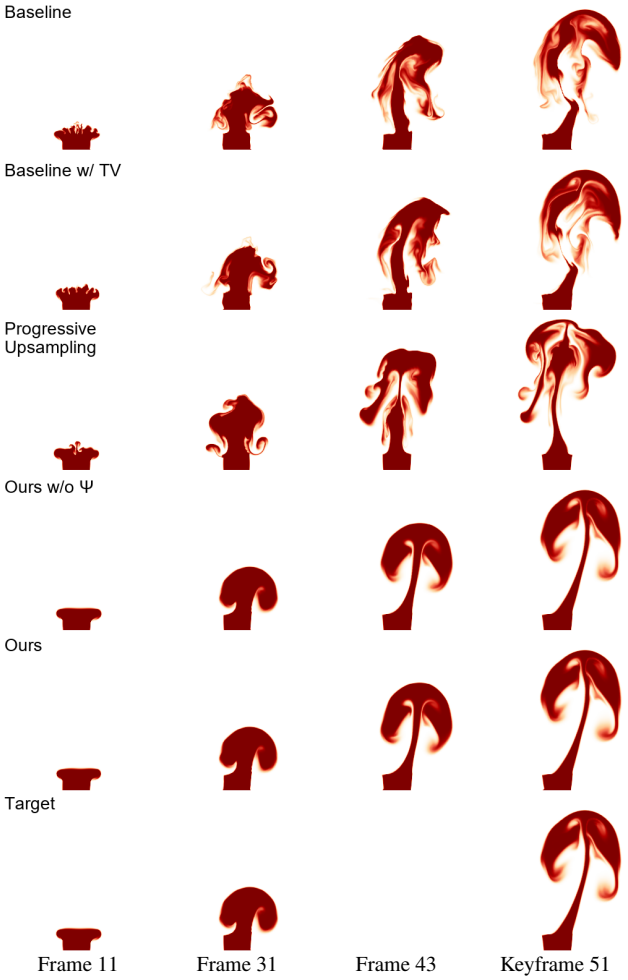

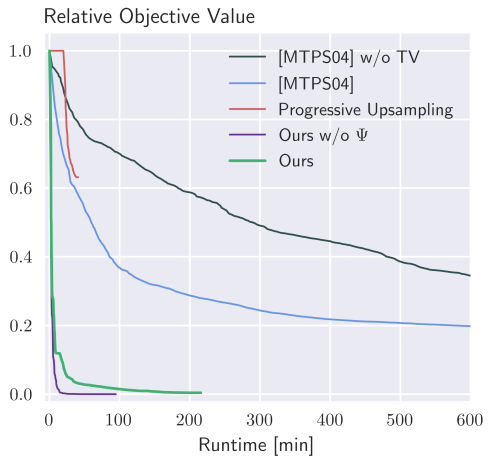

Figure 9: *uniform force* example at resolution 256^2 for different optimization schemes.

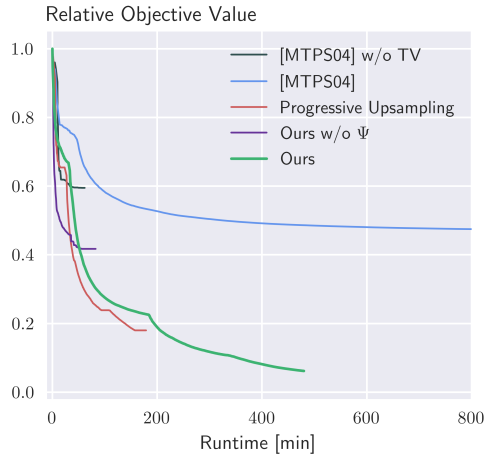

Figure 10: Convergence plot for *twist* example

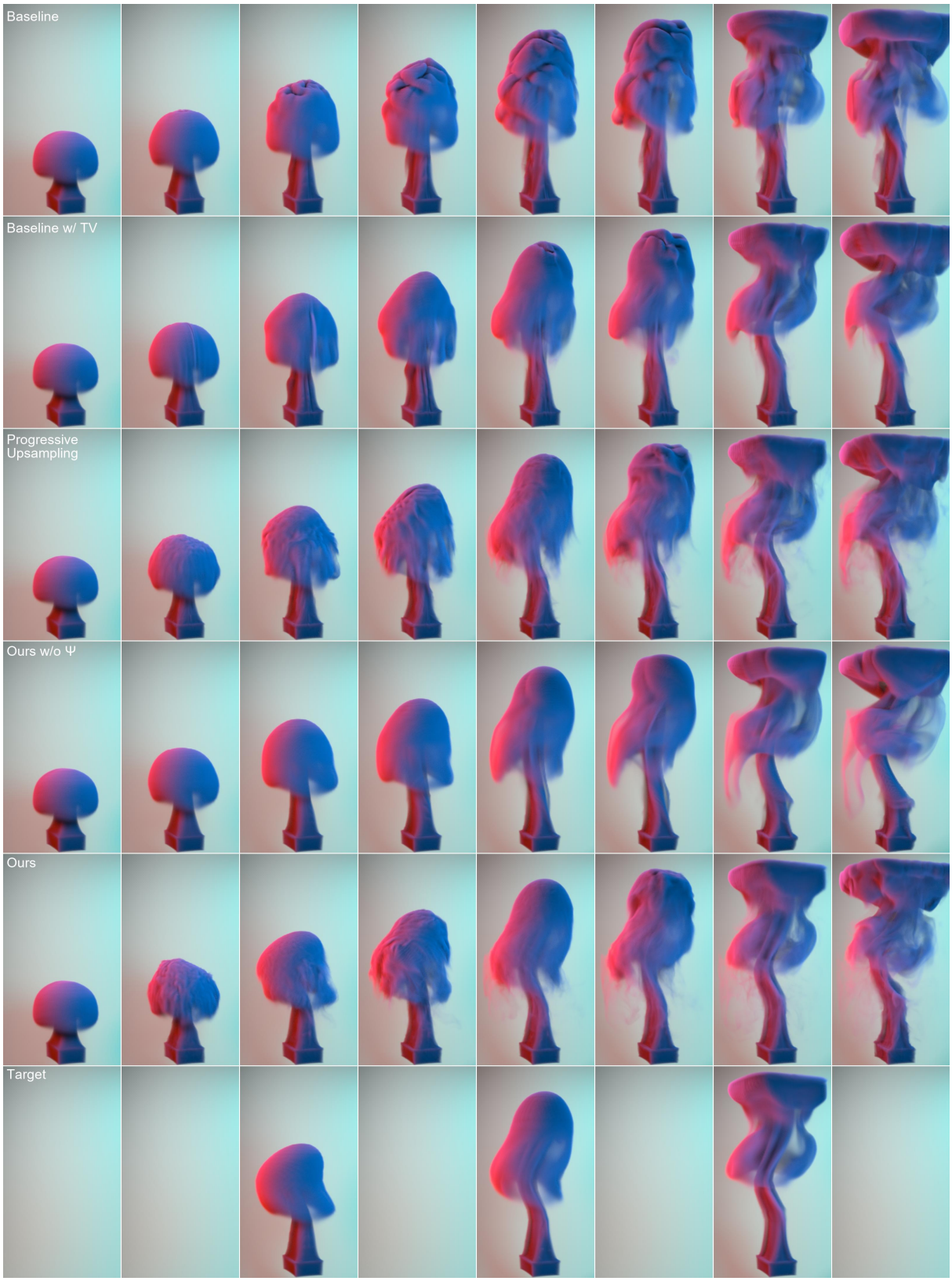

Figure 11: 3D *twist* example at resolution $100 \times 200 \times 100$ for different optimization schemes.

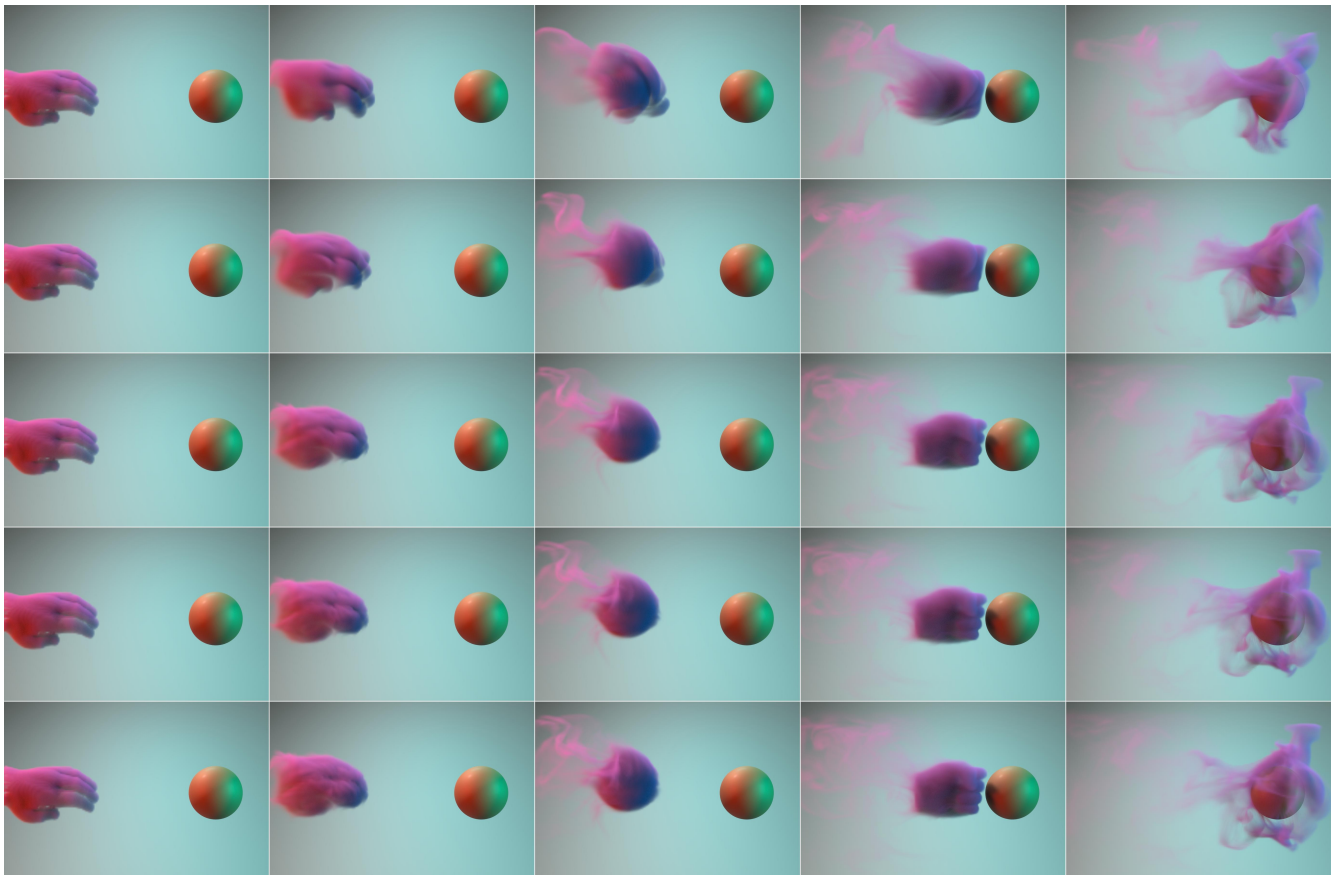

Figure 12: 3D *soft punch* example with a solid obstacle at resolution $200 \times 100 \times 100$. Two pre-defined hand shapes are used as initial frame and target frame. Our optimization results at different frequency bands are shown. From the top to the bottom, the cutoff wavenumber k_c is 1, 3, 8, 23, 64 respectively.

Figure 13: 3D *dragon* example resolution $200 \times 170 \times 60$. The density is first initialized with a dragon-shaped volume, and the letters of EG2021 are specified as target. Our optimization results at different frequency bands are shown. From the top to the bottom, the cutoff wavenumber k_c is 1, 3, 8, 23, 64 respectively.